

Research Paper

Simulation of cloud-to-ground lightning strikes to structures based on an improved stochastic lightning model

Ruijiao Jiang^{a,b}, Weitao Lyu^{a,c,*}, Bin Wu^a, Qi Qi^a, Ying Ma^a, Zhiguo Su^a, Shanshan Wu^a, Zhengshuai Xie^a, Yongbo Tan^c^a Laboratory of Lightning Physics and Protection Engineering, State Key Laboratory of Severe Weather/, Chinese Academy of Meteorological Sciences, Beijing, 100081, China^b College of Earth Sciences, University of Chinese Academy of Sciences, Beijing, 100049, China^c Key Laboratory of Meteorological Disaster, Ministry of Education (KLME), Joint International Research Laboratory of Climate and Environment Change (ILCEC), Collaborative Innovation Center on Forecast and Evaluation of Meteorological Disasters (CIC-FEMD), Key Laboratory for Aerosol–Cloud–Precipitation of China Meteorological Administration, Nanjing University of Information Science & Technology, Nanjing, 210044, China

ARTICLE INFO

Keywords:

Downward cloud-to-ground lightning
 Downward negative leader
 Upward positive leader
 Strike point
 Relative lightning frequency
 Protection distance

ABSTRACT

An improved stochastic method for computer simulation of lightning leaders is developed based on the results from optical observation data. The development and attachment process of downward negative cloud-to-ground lightning in the near-ground area is simulated. The distribution of lightning strike points influenced by tall structures is statistically analyzed. The results show that when downward negative leaders initiate at 1500 m height over a structure, the relative strike frequency for the structure increases at a decreasing rate as the structure height increases. The strike frequency for a 600 m tall structure is approximately 3.6 times that for a 100 m tall structure. Additionally, the structure may attract some lightning to hit itself and shift nearby ground strike points toward the structure. For taller structures, the deviation effect is more apparent. It is stipulated in this study that if the ground strike density in the vicinity of the structure is no more than 5% of the average density, then the structure has a sufficient protective effect on this area. The data indicate that there is a positive correlation between the protection distance and the height of the structure. The protection distances of structures of 100–600 m in height are 200 m, 280 m, 350 m, 400 m, 450 m, and 480 m approximately, which show a declining rate of increase.

1. Introduction

Lightning is a strong, long-distance, transient discharge phenomenon in the atmosphere. A thorough understanding of the physical processes and mechanisms of lightning is needed for science-based protection against lightning disasters. An effective way to study the physical mechanisms of lightning is by modeling the electrification and discharge process based on observations. At present, there are two main types of lightning leader models, the physical model and the stochastic model. Complex factors, such as the shape of the leader tip and the induced charge in the channel and corona region, should be taken into account in the physical model (Becerra and Cooray, 2006; Goelian et al., 1997; Helsdon and Farley, 1987; Mazur and Ruhnke, 1998; Mazur et al., 2000). However, these properties are difficult to obtain. By comparison,

the stochastic model has fewer factors to consider and is easier to implement. To a certain extent, it is more in agreement with the leader branching and tortuous characteristics often seen with lightning. The stochastic model was originally used to simulate the breakdown process in dielectrics, in which a pending development point is chosen randomly from among those grid points where the magnitude of the electric field is above a threshold value instead of being assigned to the grid point with the maximum electric field magnitude (Wiesmann and Zeller, 1986). The stochastic model was then used to simulate the discharge process of lightning (MacGorman et al., 2001; Petrov and Petrova, 1999). Mansell et al. (2002), Tan et al. (2006), Rioussat et al. (2007), Tao et al. (2009) and Iudin et al. (2017) used the stochastic lightning model to investigate the development of bidirectional positive and negative lightning leaders in a domain of varying charge density. The simulation results were

* Corresponding author. Laboratory of Lightning Physics and Protection Engineering, State Key Laboratory of Severe Weather/, Chinese Academy of Meteorological Sciences, Beijing 100081, China.

E-mail address: lyuwt@foxmail.com (W. Lyu).

<https://doi.org/10.1016/j.jastp.2020.105274>

Received 26 August 2019; Received in revised form 23 March 2020; Accepted 25 March 2020

Available online 8 April 2020

1364-6826/© 2020 Elsevier Ltd. All rights reserved.

supported by the observations of very high frequency radiation sources, electric field variations or camera images for the factors of channel structure, extended range, and induced charge. The above studies mostly focused on intracloud (IC) lightning, while cloud-to-ground (CG) lightning is more harmful to human society. Some researchers have applied it to the research of the interactions between CG flashes and protruding objects on the ground (Dellera and Garbagnati, 1990). Rizk (1994) fitted the relationship between the protective distance of the structure with its effective height, the length of the lightning rod, electric field and channel current respectively. Dul'zon et al. (1999) simulated the propagation of CG lightning including the initiation of lightning, a preliminary discharge in a cloud, the propagation of a downward moving stepped leader toward the earth, and the initiation and motion of an upward leader from the earth's surface. Based on this, they studied the influence of cloud charge density and channel electric parameters on the temporal and spatial characteristics of CG lightning, current and charge distribution in the channel. Some other studies combined the stochastic lightning model with the electrogeometrical model to calculate the strike distribution of the top of the low structures and the nearby ground. The results show that the top of the lightning rod and the corners of the structure are easy to be struck by lightning, while the area of the roof near the lightning rod and the ground near the structure are unlikely to be hit (Ait-Amar and Berger, 2005; Kern et al., 2012; Metwally and Heidler, 2007). It is also an effective way to study the impact of the structure on the CG lightning characteristics by simulating the development and attachment process of leaders when setting aside the charge structure of thunderstorm cloud and simply regarding the bottom of the thunderstorm as a parallel plate electrode. It was found that the probability of lightning striking a structure is closely related to the height, shape, and location of the structure (Cooray et al., 2014; He et al., 2009; Petrov et al., 2003; Petrov and Waters, 1995).

When thunderstorm clouds are present, the local electric field at the tips or corners of tall structures increases, which makes the tall structures more susceptible to lightning, while the probability of lightning striking the surrounding low structures or the flat ground becomes relatively smaller. At present, there are few studies on the impacts of tall structures on lightning activities in their vicinities. Ngqungqa (2006) analyzed the lightning activities around two iron towers in South Africa using data obtained from Eskom's lightning positioning and tracking system. It was found that the flash density within a 2.5 km radius of the tower was greater than that in the 2.5–10 km ring area, suggesting that the tower had attracted lightning. By comparing the lightning location data of a thunderstorm day derived from the National Lightning Detection Network with the current measurement data on the Canada's National Tower (the CN Tower), Hussein et al. (2010) found that if the number of return strokes on the CN Tower was deducted, the stroke density near the tower was lower than that further away from the tower. They argued that the CN Tower attracted flashes around the tower, which led to a decrease in the nearby flash density. Based on the detection data of the Lightning Location System of the Guangdong Power Grid Corporation, Zhang et al. (2017) investigated the distribution of CG flashes within a 10 km radius near the Canton Tower, and similar conclusions were drawn. However, there are some deviations in the results of ground lightning locations, and it is difficult to distinguish lightning strikes to tall structures from those to the ground within a certain range. Moreover, it is laborious to obtain sufficient data from observations to analyze the effects of different factors on the lightning strike process.

Modeling the discharge process of lightning can compensate for the defects of low resolution, limited sample size, and difficulty in analyzing the effects of the parameters on the results. At present, there are relatively few studies on the stochastic model for CG flash leaders, and the leader development schemes are quite different from the actual discharge process. Given this, we make some changes to the existing two-dimensional stochastic model based on optical observations. The development and attachment process of downward negative CG flash

under the influence of structures are simulated, and the lightning strike rates of structures at different heights and the distributions of ground strike points in the vicinity are analyzed.

2. Model description

The discharge scheme is constructed on the basis of Dul'zon et al. (1999), Petrov et al. (2003), He et al. (2009) and Tan et al. (2014a). A certain extent of rectangular space above the ground is regarded as the research domain, in which we simulate the development of downward negative lightning, which constitutes over 90% of all CG lightning (Rakov and Uman, 2003). The vertical range of the domain is 1500 m, and the horizontal range is adjusted according to the specific situation. The grid resolution is 10 m × 10 m. Each step of the leader develops at the intersection of the grids.

A thunderstorm cloud generates the background electric field in the simulated domain. The bottom of the thunderstorm cloud and the ground can be regarded as parallel plate capacitors when with the absence of any structure, and the potential of the ground is 0 V. Given the corona produced by the tips of artificial structures and trees, the field strength at the ground-level is set at −5 kV/m and the field strength at the top boundary is set at −90 kV/m, with the exponential trend among them (Biagi et al., 2011). The initial position of the downward negative leader (DNL) is fixed at the top center of the simulated domain, and the DNL has an initial length of 40 m in a vertically downward direction. In the simulations, the leader channel is assumed to be completely ionized and that the potential of the DNL does not change with channel development. The potential of the DNL is −40 MV, which is similar to the assumption in Mazur et al. (2000), Rioussset et al. (2007), Tan et al. (2014b). A rectangular structure is set at the bottom of the domain, whose potential is 0 V. The upward leader could either initiate from the structure or the ground, so the potential is also set to be 0 V. The leader, structure, and ground are defined to satisfy the Dirichlet boundary condition, where the potential is constant. The air boundary satisfies the Neumann boundary condition, where the normal derivative of the potential is constant. The atmospheric electric field distribution around the building is calculated using Laplace's equation. The successive over-relaxation iterative algorithm is used to solve Laplace's equation under the given boundary conditions in the discretization field.

As observed, the DNL can produce many branches, while the upward positive leader (UPL) generally has no obvious branching in the near-ground region (Jiang et al., 2015; Jiang et al., 2014; Krider and Ladd, 1975; Krider and Wetmore, 1987; Lu et al., 2013; Lu et al., 2012; Lu et al., 2016; Qi et al., 2018; Saba et al., 2017). Thus, in the model, each developed point of the DNL can develop to a nearby undeveloped point. The probability formula can be used to calculate the probability of each possible breakdown step (see formula (1) in Mansell et al. (2002)). The next step of the DNL is selected randomly according to the weight of the probability (MacGorman et al., 2001; Mansell et al., 2002). To avoid the branching of the UPL in the model, only the tip of UPL can develop to one of the undeveloped points around it. According to the observation (Becerra and Cooray, 2008; Saba et al., 2017), we set the speed ratio of DNL to UPL as 4:1, that is, when DNL develops four steps, UPL develops one step. A general consensus exists in the present literature that values around 100–500 kV/m is a reasonable estimate of fields needed for leader initiation (Becerra and Cooray, 2008; Gurevich and Zybin, 2001, Helsdon et al., 2002; MacGorman et al., 2001; Mansell et al., 2005; Petrov et al., 2003; Rioussset et al., 2007). This research adopts a threshold of 400 kV/m for the initiation of UPL (Helsdon et al., 1992; Helsdon and Farley, 1987; MacGorman et al., 2001). As we only simulate the near-ground part of DNL, so the initiation of DNL is not involved. In general, the initiation threshold of leader is larger than its propagation threshold (Helsdon and Farley, 1987; Judin et al., 2017; MacGorman et al., 2001; Williams et al., 1985), which is accordingly set as 150 kV/m (Griffiths and Phelps, 1976; Helsdon et al., 1992; MacGorman et al., 2001; Tan et al., 2006; Tao et al., 2009; Williams et al., 1985). The

attachment threshold between the DNL and UPL is set as 500 kV (Ait-Amar and Berger, 2005; Becerra and Cooray, 2008). Indeed, the choice of discharge parameters is somewhat subjective, given the uncertain of the charge distribution in the channel and space and other facts in the actual discharge process. However, the values above are reasonable based on the previous research.

Fig. 1 shows the spatial schematic diagram for the simulations. The width of the structure is 40 m, and its height ranges from 100 to 600 m, with an interval of 100 m. In the figure, structures at different heights are marked as colored rectangles. The horizontal distance between the structure and the DNL initial point ranges from 0 to 2000 m, also with an interval of 100 m. When the horizontal distance ranges from 0 to 1500 m, the simulation area is 4000 m × 1500 m, as shown in Fig. 1(a). When the distance ranges from 1600 to 2000 m, the simulation area is 5000 m × 1500 m, as shown in Fig. 1(b). This method not only reduces the computing time but also creates enough space between the structure and the air boundary, thus eliminating the influence of the boundary. There are a total of 126 schemes, and each is simulated 400 times to obtain statistically significant results. To simplify the description below, we set the abscissa of the structure's central axis to 0 for each scheme. Correspondingly, the abscissa of the DNL or strike point is the horizontal distance between the DNL or strike point and the structure. In the figure, the abscissa of the leftmost structure is set as 0.

3. Results and discussion

3.1. Simulation results

Using the scheme that the height of the structure is 600 m and the horizontal position of the DNL initial point is 1000 m as an example, the simulation results of four flashes are shown in Fig. 2. The initial point of the UPL connected with the DNL is the lightning strike point. According to the location of the strike point, the simulation results can be divided into three cases, each of which is supported by the Tall-Object Lightning Observatory in Guangzhou (TOLOG) observations. The Canton Tower, whose height is 600 m, is the tallest structure in the TOLOG observation area. This study uses the Canton Tower as a reference and shows several high-speed video camera images (10,000 fps) corresponding to the simulation results.

The first case is that the strike point is at the top of the structure. Fig. 2(a and b) shows the simulation results for two flashes. The tip of the DNL connects to the tip of the upward connecting leader (UCL) (hereafter called tip-to-tip attachment) in Fig. 2(a). The tip of the DNL connects to the lateral of the UCL (hereafter called tip-to-lateral attachment) in Fig. 2(b) (Kostinskiy et al., 2016; Lu et al., 2013; Lu et al., 2016). The

ratio of two types of attachment when lightning hit the structure is close to 50%, no matter where is the DNL initial point, which is similar to the observation in Lu et al. (2016). An enlarged view of the leader attachment in the dashed frame is shown in the solid line frame. TOLOG has obtained images of these two attachment patterns on many occasions. Fig. 3(a and b,c,d) are high-speed photographs before and after two strokes hitting the Canton Tower. We set the first frame of the beginning of the return stroke to zero hour, and the corresponding times of the four frames are marked in the figures. By comparing the discharge channel before and after the return stroke, we can determine that Flash-1 is of tip-to-tip attachment and that Flash-2 is of tip-to-lateral attachment.

The second case is when lightning strikes the side of the structure, where the length of the UCL is much shorter than that in the first case, and the top of the structure may generate a long unconnected upward leader (UUL), as shown in Fig. 2(c). In the study, side flashes only occur sporadically on structures over 300 m, and there is no case of tip-to-lateral attachment. For the observations of TOLOG over many years, only one side flash striking the Canton Tower has been obtained, as Flash-3 shown in Fig. 3(e).

The third case is that the lightning does not hit the structure, but hits the nearby ground also of only tip-to-tip attachment in this case, as shown in Fig. 2(d). In this case, the UCL is relatively short (Jiang et al., 2015; Krider and Ladd, 1975). If the DNL is close to the structure, then it can also trigger a long UUL from the structure (Krider and Wetmore, 1987), as shown in Flash-4 in Fig. 3(f,g,h).

3.2. Analysis of lightning strikes to the structure

In this paper, the lightning strike probabilities (the number of lightning strikes to the structure versus the number of simulations) for structures at different heights when the DNL initial point ranges from 0 m to 2000 m are calculated. Six curves of lightning strike probability with the location of the DNL initial point are fitted, as shown in Fig. 4. For structures at all heights, the strike probability decreases with increasing distance. When the DNL initiates directly above the structure, the strike probability for a 100 m and 200 m tall structure is 94% and 98% respectively, and the probability for other heights is 100%. When the lightning strike probabilities of all structures decrease to 50%, the corresponding DNL initial points are approximately 620 m, 880 m, 1040 m, 1170 m, 1270 m, and 1350 m. When the strike probability is between 20% and 80%, the curve decreases nearly linearly, and the absolute value of the decline rate increases with the height of the structure. With the increase of the DNL initial point, the intervals between the lines first increase and then decrease. It means the height of the structure matters little to the strike probability when the DNL is on the top of the structure or very far away from the structure. In the middle distances, the height has the greatest influence on the strike probability.

To analyze the comprehensive cases of lightning strikes to the structure when flashes are generated evenly, we integrate the lightning strike probability within a radius of 2 km around the structure using formula (1) based on the fitted results with the logistic model. Formula (1) is as follows:

$$N = \int_0^2 f(r) \cdot 2\pi r \cdot dr, \quad (1)$$

where r (km) is the distance between the DNL initial point and the structure, $f(r)$ is the lightning strike probability for the structure when the DNL initiates at a distance of r , and N is the relative lightning strike frequency for the structure.

The relative lightning strike frequencies for the structures, when the average lightning density is 1 km^{-2} , are shown in Fig. 5. According to the trend of the curves, the relative frequency is positively correlated with the height of the structure. However, this is not a simple linear positive correlation, but with an increase of structure height, the rate of change of the curve decreases, which corresponds to the variations in the

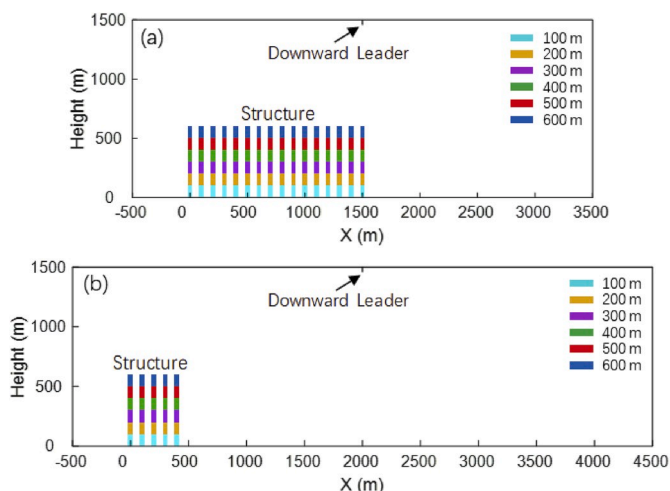


Fig. 1. Spatial schematic diagram of the simulations.

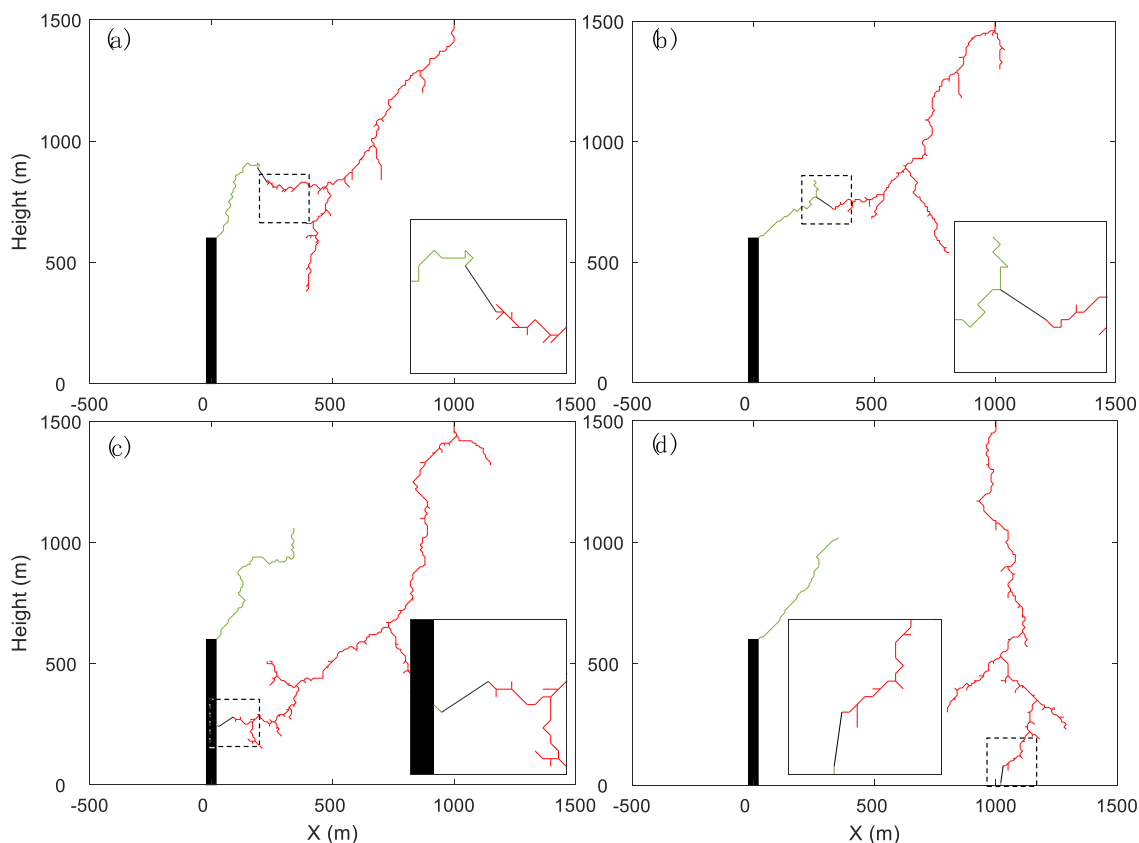


Fig. 2. Simulation Results: (a) A flash strikes the top of the structure with a tip-to-tip attachment; (b) A flash strikes the top of the structure with a tip-to-lateral attachment; (c) A flash strikes the side of the structure with a tip-to-tip attachment; (d) A flash strikes the ground with a tip-to-tip attachment. The structure is represented by the black rectangle. The red lines and the green lines are branches of the DNL and UPL, respectively. The black line is the attachment process after the potential difference between them reaches the attachment threshold. (For interpretation of the references to color in this figure legend, the reader is referred to the Web version of this article.)

spacing between the curves with the increase of structure height in Fig. 4. Relative lightning strike frequencies of structures at 100–600 m are 1.7, 2.8, 3.8, 4.6, 5.3 and 5.9, respectively. The probability of a 600 m structure being hit by downward negative CG lightning is approximately 3.6 times that of a 100 m structure.

3.3. Analysis of lightning strikes to the ground

Fig. 6 shows the distributions of ground strike points when the DNL initial points are at different positions. The heights of the structures are 100 m and 600 m in Fig. 6(a) and (b), respectively. For the cases when few lightning flashes (less than 10) strike the ground or some points strike the other side of the structure, the locations of the ground strike points are shown by diamonds in the figure. The red dots in the figure are the averages of the ground strike points. For comparison, the theoretical averages of the ground strike point positions when the structure does not exist are also marked by the black dots in the figure. In the absence of the structure, the ground strike points present a normal distribution centered on the abscissa of the DNL initial point, so the horizontal and vertical coordinates of all black points are the same.

When the height of the structure is 100 m and the DNL initial point is right above the central axis of the structure, there are 23 strikes on the ground, which show an approximately symmetrical distribution centered on the structure. When the DNL initial point is 100 or 200 m, there are also separate ground strike points on the other side of the structure. The average of the ground strike point positions is not calculated when the DNL initial point ranges from 0 m to 400 m. When the DNL initial point is 500 m or more, the ground on only one side of the structure is hit. As the distance between the DNL initial point and the

structure increases, the distribution range of the ground strike points gradually expands. When the DNL initial point is close, the value of the red point is larger than the black point's, and the distance between the red point and the black point is greater, being approximately 300 m. This means that the average of the ground strike points is farther from the structure than the DNL initial point. As the distance between the DNL initial point and the structure increases, the two points approach and gradually coincide.

For the case that the structure is 600 m high and only when the distance between the DNL initial point and the structure is more than 600 m, lightning can potentially strike the ground. When the DNL initial point is close, the value of the red point is smaller than the black point's, and the distance between them is approximately 200 m. Same with the first case, the two points gradually coincide with each other with an increase in the distance between the DNL initial point and the structure. To make a more intuitive comparison, only the tallest and lowest cases of structures are drawn. When the height of the structure is between these cases, the position of the red dot is transitional.

To explain why the averages of the ground strike points of structures at different heights show this discrepancy, more detailed distributions of the ground strike points in the vicinities of the two structures at 100 m and 600 m when the DNL initial point is at a certain location are shown in Fig. 7. The ordinate is the proportion of the number of samples per interval. In Fig. 7(a), the height of the structure is 100 m, and the DNL initial point is 500 m. A total of 142 flashes strike the ground. In Fig. 7 (b), the height of the structure is 600 m, and the DNL initial point is 1000 m. A total of 50 flashes strike the ground. The formulation of the scheme in the figure is that the DNL initial point is the nearest when the number of ground strike points is over 50 and they only hit one side of

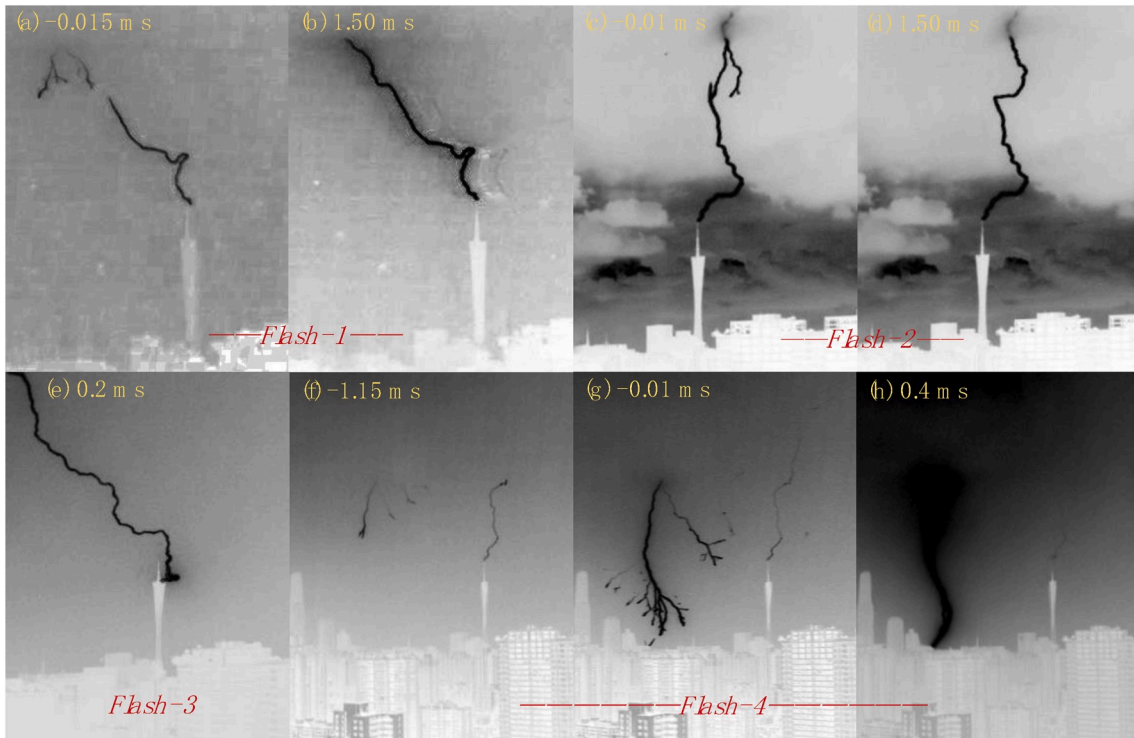


Fig. 3. (a,b) A flash strikes the top of the Canton Tower with a tip-to-tip attachment; (c,d) A flash strikes the top of the Canton Tower with a tip-to-lateral attachment; (e) A flash strikes the side of the Canton Tower; (f,g,h) A flash strikes the lower structure near the Canton Tower with a tip-to-tip attachment.

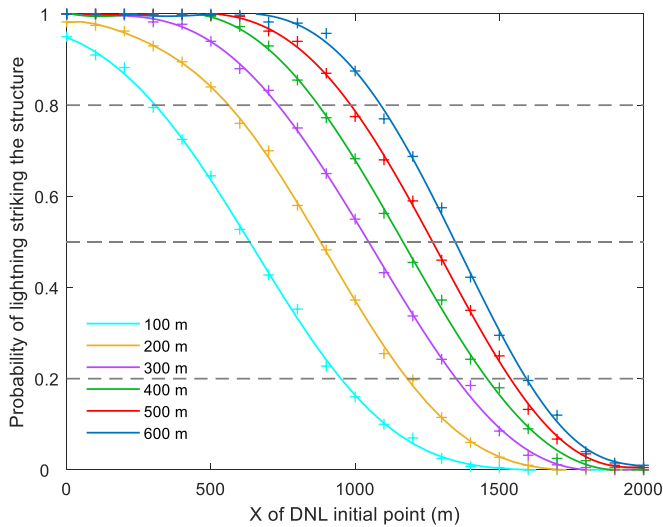


Fig. 4. Lightning strike probabilities of structures at six heights with the positions of the DNL initial points.

the ground. In this way, not only is there statistical significance but also the contrast is more obvious. The lightning striking the ground is represented by a bar chart with a solid red border, and the lightning striking the structure is represented by a bar chart with a dashed red border. At the same time, the distribution of ground strike points when the structure does not exist is shown by the gray bar chart. The gray bar graph is obtained by setting the height of the structure to 0 m and running 2000 simulations. The distribution is approximately normal, and the range is slightly greater than 2000 m. In Fig. 7(a), the right-side red solid line bar graph is highly consistent with the gray bar graph, while the rest are generally smaller than the gray bar graph. This means that the lower structure tends to attract left-leaning ground strike points to the

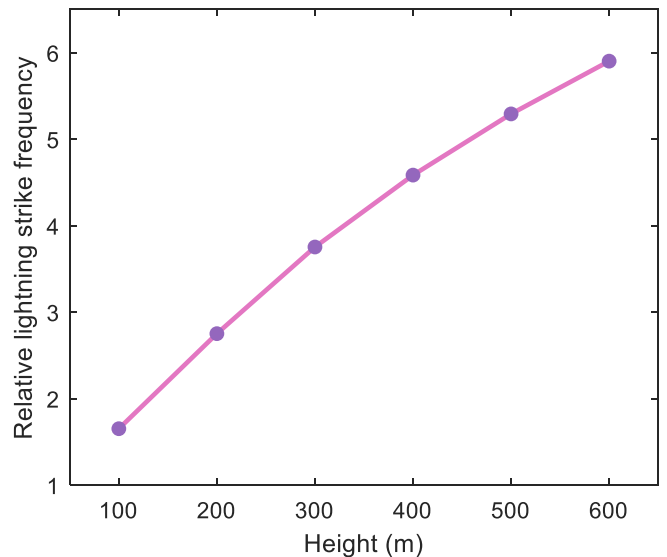


Fig. 5. Relative strike frequencies for the structures at six heights by downward negative CG lightning when the DNL initial points are evenly distributed at a height of 1500 m with the density of 1 km^{-2} .

structure, retaining the points that are relatively further such that the average of the positions of the ground strike points is larger than when there is no structure. In Fig. 7(b), the position of the red solid line bar graph is to the left of the gray bar graph, so the average of the positions of the ground strike points is smaller than when there is no structure. It shows that the tall structure attracts a portion of the flashes to itself, and that others striking the ground are attracted toward the structure. When the structure is low, it has little influence on the ground strike points. The taller the structure is, the greater the deviation of the ground strike points toward the structure.

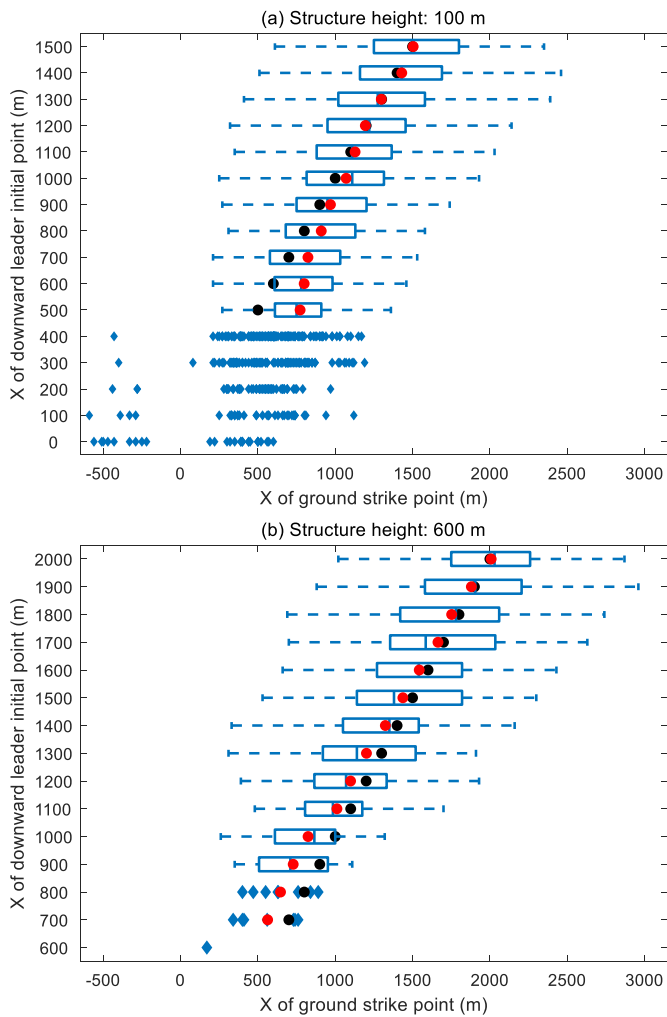


Fig. 6. The distributions of ground strike points when the initial DNL point is at different positions. (a) The height of the structure is 100 m. (b) The height of the structure is 600 m. The diamonds and boxes are the distributions of ground strike points. The red points are the averages of the ground strike points in the presence of the structure. The black points are the averages of ground strike points in the absence of the structure. (For interpretation of the references to color in this figure legend, the reader is referred to the Web version of this article.)

A figure of potential spatial distribution at the initiation of DNL can be more intuitive to illustrate the attraction effect of the structure, as shown in Fig. 8. In this case, the height of the structure is 600 m and the DNL initial point is at 1000 m. It can be seen that on the left side of the DNL, namely the side containing the structure, the equipotential lines are denser than the side without the structure and the field strength is greater, which is more conducive to the development of the leader.

By superimposing the ground strike points when the DNL initial points are at different positions, the one-dimensional lightning density distribution on the ground near the structure can be obtained when the flashes are generated evenly at a height of 1500 m. When the abscissa of the DNL initial point exceeds 2000 m, it can be assumed that the positions of the ground strike points are no longer affected by the structure, so in this case, the normal distribution (gray bar graph) in Fig. 7 is superimposed at each distance. As the lightning distribution in the vicinity of an isolated structure is centrosymmetric, the two-dimensional lightning density can be obtained by rotating the one-dimensional distribution curve (after smooth interpolation) around the structure. The average density of the ground strike points is converted to 1 km^{-2} . Fig. 9 shows the distribution of lightning around the structure with 600 m

height. At approximately 3000 m from the structure, the density of lightning on the ground tends to 1 km^{-2} . As the distance from the structure decreases, the density of lightning on the ground gradually decreases.

Fig. 10 shows the two-dimensional distribution of grounding points at different distances for all structures. Owing to the attraction of the structure, the lightning density for the nearby ground is lower than average and drops to 0 at a certain close distance. Greater structure heights show lower nearby lightning densities. At the same time, the difference between the two structures with adjacent heights decreases as the height increases. It can be seen that the lightning distributions near the structures with heights of 500 m and 600 m are very close. Compared with Fig. 7, it can be inferred that this may be due to the deviation of the ground strike points near the tall structure.

This study stipulates that when the lightning density on the ground is less than 5% of the average density, the structure has a sufficient protective effect on the area. According to the six curves in Fig. 10, the protection distances of structures at the six heights are calculated to be 200 m, 280 m, 350 m, 400 m, 450 m, and 480 m, respectively, as shown in Fig. 11. With the increasing height of the structure, the protection distance increases, but the rate of change of the curve decreases, which corresponds to the decreases in the differences between the curves in Fig. 10. The trend of the curve is consistent with the previous research summarized in Golde (1977).

4. Conclusions

Based on the two-dimensional stochastic lightning leader model, this study adopts a discharge plan that is in agreement with observations. The structures distort the spatial electric field and affect the channel of lightning. By simulating the development and attachment process of downward negative CG lightning when the DNL initial points are at different positions and the structures are at different heights, the horizontal positions of the ground strike points for different schemes are computed. The one-dimensional distribution of the grounding points is transformed into a two-dimensional distribution through a certain spatial transformation relationship. On this basis, the relative lightning strike frequencies for structures at different heights, the distributions of the lightning strike points and the protection distances on the surrounding ground of structures are determined. In this paper, some quantitative conclusions are reached, which can improve the understanding of the physical process of lightning and the interaction between flashes and objects.

The lightning strike rate for the structures decreases with an increase of the horizontal distance of the DNL initial point, where the decline rate first increases and then decreases. Assuming that the DNL initial points are evenly distributed at 1500 m height, the relative lightning strike frequencies of structures at 100–600 m are 1.7, 2.8, 3.8, 4.6, 5.3 and 5.9, respectively, when the average lightning density on the ground is 1 km^{-2} . The relative lightning strike frequency for the structures increases with increasing structure height, but the rate of increase decreases with increasing structure height.

By analyzing the distribution of the ground strike points, it is found that tall structures attract the ground strike points toward the structure and that the deviation is positively correlated with the height of the structure. By superimposing the simulated positions of the ground strike points, the distribution in the vicinity of the structure and the protection distance on the surrounding ground of the structure can be obtained. The protection distance is positively correlated with the height of the structure, but the rate of increase decreases with the height of the structure. According to the definition of protection distance in this paper, the protection distances of structures at 100–600 m are 200 m, 280 m, 350 m, 400 m, 450 m, and 480 m, respectively.

In this paper, the development and attachment process of DNL and UPL are well simulated, which is close to the observed results.

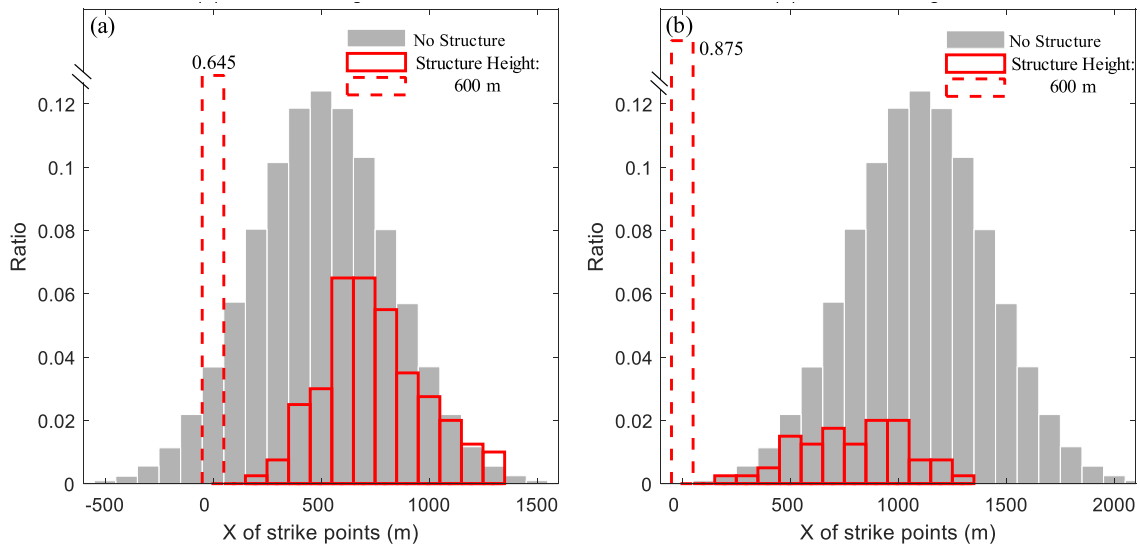


Fig. 7. Distribution of ground strike points in the presence of the structure (red line bar) and the absence of the structure (gray bar). (a) The height of the structure is 100 m, and the DNL initial point is 500 m. (b) The height of the structure is 600 m, and the DNL initial point is 1000 m. (For interpretation of the references to color in this figure legend, the reader is referred to the Web version of this article.)

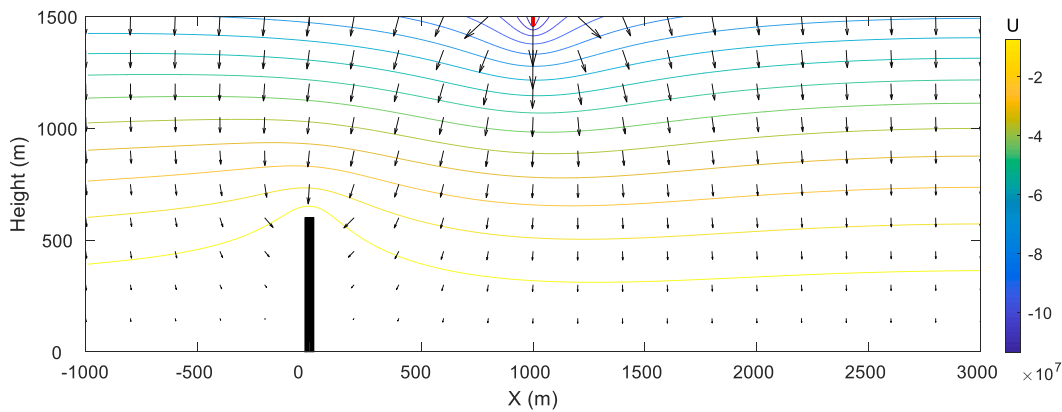


Fig. 8. Potential spatial distribution during the process of lightning. The arrows represent the magnitude and direction of the electric field.

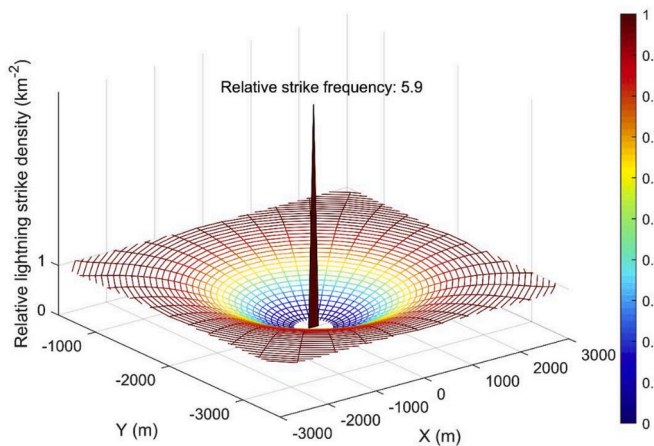


Fig. 9. The 2-D relative density of ground strike points of downward negative CG flashes near the structure with 600 m height, and the relative frequency of CG flashes hitting the structure when the DNL initial points are evenly distributed at a height of 1500 m. The central peak represents the relative frequency of the structure.

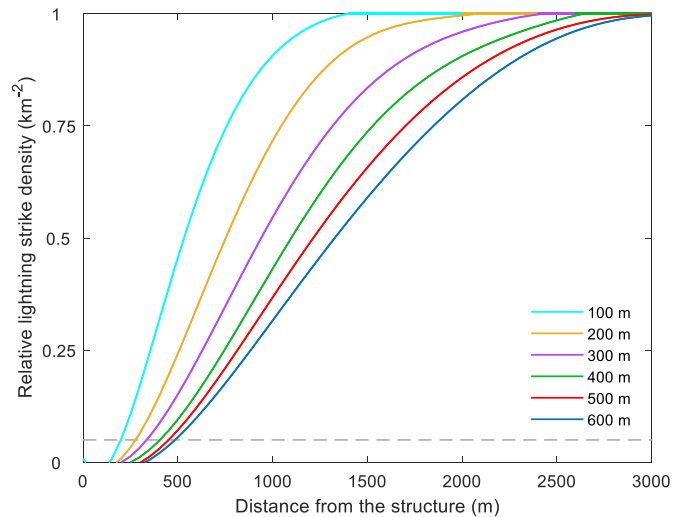


Fig. 10. The 2-D relative density of ground strike points of downward negative CG flash near the structure at six heights.

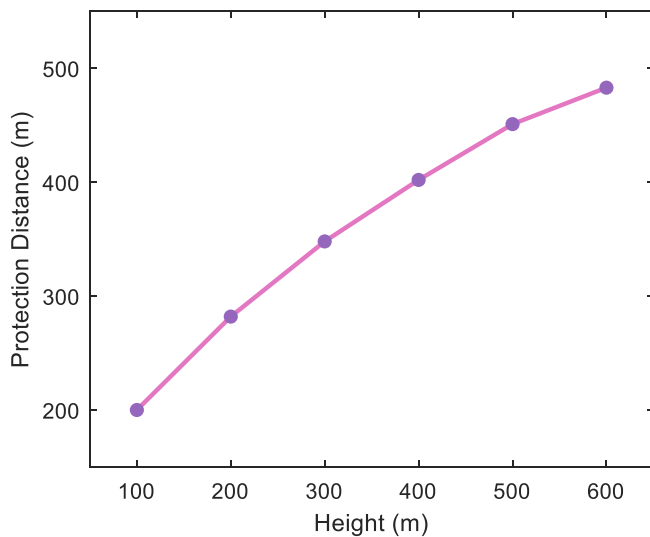


Fig. 11. Protection distances of the structures with six heights.

Additionally, each scheme is simulated multiple times, and some laws having statistical significance are calculated. At the same time, the conversion method in this paper can effectively reduce the enormous calculations from direct use of a three-dimensional model to simulate the distribution on a horizontal plane. However, for the simulations in this study, a series of more complex problems, such as a change in leader speed in the process of development, the phenomena of double or multiple ground points, the influence of structural shape, and the comprehensive effects of structure group, have not been taken into account, which needs further research.

Acknowledgments

This work was supported in part by the National Key Research and Development Program of China under grant 2017YFC1501504 and the National Natural Science Foundation of China under grants 41775010. Thanks for the helpful and valuable suggestions from two anonymous reviewers.

References

- Ait-Amar, S., Berger, G., 2005. Lightning interception on elevated building. In: Proc. of 5th WSEAS Int. Conf. on Power Systems & EMC, pp. 17–23.
- Becerra, M., Cooray, V., 2006. A simplified physical model to determine the lightning upward connecting leader inception. *IEEE Trans. Power Deliv.* 21 (2), 897–908.
- Becerra, M., Cooray, V., 2008. On the velocity of positive connecting leaders associated with negative downward lightning leaders. *Geophys. Res. Lett.* 35 (2).
- Biagi, C.J., Uman, M.A., Gopalakrishnan, J., Hill, J., Rakov, V.A., Ngim, T., Jordan, D.M., 2011. Determination of the electric field intensity and space charge density versus height prior to triggered lightning. *J. Geophys. Res.: Atmos.* 116 (D15).
- Cooray, V., Kumar, U., Rachidi, F., Nucci, C.A., 2014. On the possible variation of the lightning striking distance as assumed in the IEC lightning protection standard as a function of structure height. *Electr. Power Syst. Res.* 113, 79–87.
- Dellera, L., Garbagnati, E., 1990. Lightning stroke simulation by means of the leader progression model. I. Description of the model and evaluation of exposure of free-standing structures. *IEEE Trans. Power Deliv.* 5 (4), 2009–2022.
- Dul'zon, A.A., Lopatin, V., Noskov, M., Pleshkov, O., 1999. Modeling the development of the stepped leader of a lightning discharge. *Tech. Phys.* 44 (4), 394–398.
- Goelian, N., Lalande, P., Bondiou-Clergerie, A., Bacchiega, G., Gazzani, A., Gallimberti, I., 1997. A simplified model for the simulation of positive-spark development in long air gaps. *J. Phys. Appl. Phys.* 30 (17), 2441.
- Golde, R., 1977. The lightning conductor. In: Golde, R.H. (Ed.), *Lightning* 2.
- Griffiths, R., Phelps, C., 1976. The effects of air pressure and water vapour content on the propagation of positive corona streamers, and their implications to lightning initiation. *Q. J. R. Meteorol. Soc.* 102 (432), 419–426.
- Gurevich, A.V., Zybin, K.P., 2001. Runaway breakdown and electric discharges in thunderstorms. *Phys. Usp.* 44 (11), 1119.
- He, J., Zhang, X., Dong, L., Zeng, R., Liu, Z., 2009. Fractal model of lightning channel for simulating lightning strikes to transmission lines. *Sci. China E* 52 (11), 3135.

- Helsdon, John, H., Wu, G., Farley, R.D., 1992. An intracloud lightning parameterization scheme for a storm electrification model. *J. Geophys. Res. Atmos.* 97 (D5), 5865–5884.
- Helsdon, J.H., Farley, R.D., 1987. A numerical modeling study of a Montana thunderstorm: 2. Model results versus observations involving electrical aspects. *J. Geophys. Res.: Atmos.* 92 (D5), 5661–5675.
- Helsdon Jr., J.H., Gattaleeradapan, S., Farley, R.D., Waits, C.C., 2002. An examination of the convective charging hypothesis: charge structure, electric fields, and Maxwell currents. *J. Geophys. Res.: Atmos.* 107 (D22), ACL 9-1–ACL 9-26.
- Hussein, A., Jan, S., Todorovski, V., Milewski, M., Cummins, K., Janischewskyj, W., 2010. Influence of the CN Tower on the lightning environment in its vicinity. In: *Proceedings of the International Lightning Detection Conference (ILDC)*, pp. 1–19.
- Iudin, D.I., Rakov, V.A., Mareev, E.A., Iudin, F.D., Syssoev, A.A., Davydenko, S.S., 2017. Advanced numerical model of lightning development: application to studying the role of LPCR in determining lightning type. *J. Geophys. Res.* 122 (12).
- Jiang, R., Qie, X., Wang, Z., Zhang, H., Lu, G., Sun, Z., Liu, M., Li, X., 2015. Characteristics of lightning leader propagation and ground attachment. *J. Geophys. Res.: Atmos.* 120 (23), 11,988–912,002.
- Jiang, R., Qie, X., Wu, Z., Wang, D., Liu, M., Lu, G., Liu, D., 2014. Characteristics of upward lightning from a 325-m-tall meteorology tower. *Atmos. Res.* 149, 111–119.
- Kern, A., Schelthoff, C., Mathieu, M., 2012. Probability of lightning strikes to air-terminations of structures using the electro-geometrical model theory and the statistics of lightning current parameters. *Atmos. Res.* 117 (Complete), 2–11.
- Kostinskiy, A.Y., Syssoev, V.S., Bogatov, N.A., Mareev, E.A., Andreev, M.G., Bulatov, M. U., Makal'sky, L.M., Sukharevsky, D.I., Rakov, V.A., 2016. Observations of the connection of positive and negative leaders in meter-scale electric discharges generated by clouds of negatively charged water droplets. *J. Geophys. Res.: Atmos.* 121 (16), 9756–9766.
- Krider, E., Ladd, C.J.W., 1975. Upward streamers in lightning discharges to mountainous terrain. *Weather* 30 (3), 77–81.
- Krider, E.P., Wetmore, R.H., 1987. Upward streamers produced by a lightning strike to radio transmission towers. *J. Geophys. Res.: Atmos.* 92 (D8), 9859–9862.
- Lu, W., Chen, L., Ma, Y., Rakov, V.A., Gao, Y., Zhang, Y., Yin, Q., Zhang, Y., 2013. Lightning attachment process involving connection of the downward negative leader to the lateral surface of the upward connecting leader. *Geophys. Res. Lett.* 40 (20), 5531–5535.
- Lu, W., Chen, L., Zhang, Y., Ma, Y., Gao, Y., Yin, Q., Chen, S., Huang, Z., Zhang, Y., 2012. Characteristics of unconnected upward leaders initiated from tall structures observed in Guangzhou. *J. Geophys. Res.: Atmos.* 117 (D19).
- Lu, W., Qi, Q., Ma, Y., Chen, L., Yan, X., Rakov, V.A., Wang, D., Zhang, Y., 2016. Two basic leader connection scenarios observed in negative lightning attachment process. *High Voltage* 1 (1), 11–17.
- MacGorman, D.R., Straka, J.M., Ziegler, C.L., 2001. A lightning parameterization for numerical cloud models. *J. Appl. Meteorol.* 40 (3), 459–478.
- Mansell, E.R., MacGorman, D.R., Ziegler, C.L., Straka, J.M., 2002. Simulated three-dimensional branched lightning in a numerical thunderstorm model. *J. Geophys. Res.: Atmos.* 107 (D9), ACL 2-1–ACL 2-12.
- Mansell, E.R., MacGorman, D.R., Ziegler, C.L., Straka, J.M., 2005. Charge structure and lightning sensitivity in a simulated multicell thunderstorm. *J. Geophys. Res.: Atmos.* 110 (D12).
- Mazur, V., Ruhnke, L.H., 1998. Model of electric charges in thunderstorms and associated lightning. *J. Geophys. Res.: Atmos.* 103 (D18), 23299–23308.
- Mazur, V., Ruhnke, L.H., Bondiou-Clergerie, A., Lalande, P., 2000. Computer simulation of a downward negative stepped leader and its interaction with a ground structure. *J. Geophys. Res.: Atmos.* 105 (D17), 22361–22369.
- Metwally, I.A., Heidler, F., 2007. Computation of collection area and probability of lightning strikes to structures using the electrogeometric model. *Eur. Trans. Electr. Power* 17 (6), 582–596.
- Ngqungqqa, S.H., 2006. A critical evaluation and analysis of methods of determining the number of times that lightning will strike a structure.
- Petrov, N., Petrova, G., D'Alessandro, F., 2003. Quantification of the probability of lightning strikes to structures using a fractal approach. *IEEE Trans. Dielectr. Electr. Insul.* 10 (4), 641–654.
- Petrov, N., Waters, R., 1995. Determination of the striking distance of lightning to earthed structures. *Proc. Roy. Soc. Lond. Math. Phys. Sci.* 450 (1940), 589–601.
- Petrov, N.I., Petrova, G.N., 1999. Physical mechanisms for the development of lightning discharges between a thundercloud and the ionosphere. *Tech. Phys.* 44 (4), 472–475.
- Qi, Q., Lyu, W., Wu, B., Ma, Y., Chen, L., Liu, H., 2018. Three-dimensional optical observations of an upward lightning triggered by positive cloud-to-ground lightning. *Atmos. Res.* 214, 275–283.
- Rakov, V.A., Uman, M.A., 2003. *Lightning: Physics and Effects*. Cambridge University Press.
- Rioux, J.A., Pasko, V.P., Krehbiel, P.R., Thomas, R.J., Rison, W., 2007. Three-dimensional fractal modeling of intracloud lightning discharge in a New Mexico thunderstorm and comparison with lightning mapping observations. *J. Geophys. Res.* 112 (D15).
- Rizk, F.A., 1994. Modeling of lightning incidence to tall structures. II. Application. *IEEE Trans. Power Deliv.* 9 (1), 172–193.
- Saba, M., Paiva, A., Schumann, C., Ferro, M., Naccarato, K., Silva, J., Siqueira, F., Custódio, D., 2017. Lightning attachment process to common buildings. *Geophys. Res. Lett.* 44 (9), 4368–4375.
- Tan, Y., Guo, X., Zhu, J., Shi, Z., Zhang, D., 2014a. Influence on simulation accuracy of atmospheric electric field around a building by space resolution. *Atmos. Res.* 138, 301–307.

- Tan, Y., Tao, S., Liang, Z., Zhu, B., 2014b. Numerical study on relationship between lightning types and distribution of space charge and electric potential. *J. Geophys. Res.: Atmos.* 119 (2), 1003–1014.
- Tan, Y., Tao, S., Zhu, B., 2006. Fine-resolution simulation of the channel structures and propagation features of intracloud lightning. *Geophys. Res. Lett.* 33 (9).
- Tao, S., Tan, Y., Zhu, B., Ma, M., Lu, W., 2009. Fine-resolution simulation of cloud-to-ground lightning and thundercloud charge transfer. *Atmos. Res.* 91 (2–4), 360–370.
- Wiesmann, H.J., Zeller, H.R., 1986. A fractal model of dielectric breakdown and prebreakdown in solid dielectrics. *J. Appl. Phys.* 60 (5), 1770–1773.
- Williams, E.R., Cooke, C.M., Wright, K.A., 1985. Electrical discharge propagation in and around space charge clouds. *J. Geophys. Res.: Atmos.* 90 (D4), 6059–6070.
- Zhang, C., Lu, W., Chen, L., Qi, Q., Ma, Y., Yao, W., Zhang, Y., 2017. Influence of the Canton Tower on the cloud-to-ground lightning in its vicinity. *J. Geophys. Res.: Atmos.* 122 (11), 5943–5954.